

Viscous Flow Over a Permeable Stretching/Shrinking Surface in a Nanofluid: A Stability Analysis

¹Ezad H. Hafidzuddin, ²Roslinda Nazar, ³Norihan Md. Arifin and ⁴Toan Pop

¹Centre of Foundation Studies for Agriculture Science, Universiti Putra Malaysia (UPM),
43400 Serdang, Selangor, Malaysia

²School of Mathematical Sciences, Faculty of Science and Technology,
Universiti Kebangsaan Malaysia (UKM), 43600 Bangi, Selangor, Malaysia

³Department of Mathematics and Institute for Mathematical Research,
Universiti Putra Malaysia (UPM), 43400 Serdang, Selangor, Malaysia

⁴Department of Mathematics, Babes-Bolyai University, R-400084 Cluj-Napoca, Romania
ezadhafidz@upm.edu.my

Abstract: This study deals with the boundary layer flow and heat transfer near the stagnation point on a permeable stretching/shrinking surface in a nanofluid. The nanoparticles considered in this study are copper and silver. The governing nonlinear partial differential equations are transformed into a system of nonlinear ordinary differential equations using an appropriate similarity transformation which then solved numerically to study the effect of solid volume fraction or nanoparticle volume fraction parameter ϕ of the nanofluid. Multiple solutions are found for a certain range of shrinking and suction parameters, therefore, a stability analysis is performed to determine which solution is stable and physically realizable. The effects of the governing parameters on the skin friction coefficient, the local Nusselt number and the velocity and temperature profiles were presented and discussed. It was found that the nanoparticle volume fraction substantially affects the fluid flow and heat transfer characteristics.

Key words: Boundary layer, nanofluid, heat transfer, stretching/shrinking surface, dual solutions, stability analysis

INTRODUCTION

Nanofluids is a term proposed by Choi (1995) which defined as liquids that contain suspensions of nanoparticles with the size of 1-100 nm in a base fluid. Nanofluids are expected to have superior heat transfer characteristic due to the presence of the nanoparticles that increase the thermal conductivity. There are several studies on the forced and free convection using nanofluids related with differentially heated enclosures (Khanafar *et al.*, 2003; Tiwari and Das, 2007; Abu-Nada and Oztop, 2009; Muthamilselvan *et al.*, 2010). An excellent compilation of the published papers on nanofluid can be found in the book written by Das *et al.* (2008) and the papers by Daungthongsuk and Wongwises (2007), Wang and Mujumdar (2008) Kakac and Pramuanjaroenkij (2009), Fan and Wang (2011) and Vajjha and Das (2012).

In additional, a few research papers worth mentioning here are the Cheng-Minkowycz problem for natural convective boundary layer flow in a porous medium

saturated by a nanofluid by Nield and Kuznetsov (2009) viscous flow due to a permeable stretching/shrinking sheet in a nanofluid by Arifin *et al.* (2011) and the mixed convection flow from a horizontal circular cylinder in a nanofluid by Tham *et al.* (2012). We also mention, here, two of the recent studies done by Bakar *et al.* (2017) on the rotating flow over a shrinking sheet in nanofluid using Buongiorno model and thermophysical properties of nanoliquids and Uddin *et al.* (2018) on forced convective slip flow of a nanofluid past a radiating stretching/shrinking sheet.

In this study, we extend the classical problem of stagnation-point flow of a viscous and incompressible (Newtonian) fluid on a stretching/shrinking sheet first considered by Miklavcic and Wang (2006) and Wang (2008) to the case of nanofluids using the model proposed by Tiwari and Das (2007) with two different nanoparticles, namely Copper (Cu) and silver (Ag). We also extend the research by Arifin *et al.* (2011) by performing the stability analysis in order to determine the stability of the dual solutions. It is worth mentioning that

Table 1: Thermal conductivities of various solids and liquids (Wang and Mujumdar, 2008)

Variables/Materials	Thermal conductivity (W/m-K)
Metallic solids	
Copper	401
Aluminum	237
Nonmetallic solids	
Silicon	148
Alumina (Al ₂ O ₃)	40
Metallic liquids	
Sodium (644 K)	72.3
Nonmetallic liquids	
Water	0.613
Ethylene glycol (EG)	0.253
Engine oil (EG)	0.145

the flow over a continuously stretching/shrinking surface is an important problem in many engineering processes with industrial applications such as wire drawing, hot rolling and glass-fibre production. Later, several other papers on shrinking surfaces were published such as those by Sajid *et al.* (2008), Noor and Hashim (2009), Nazar *et al.* (2011), Bhattacharyya *et al.* (2013) and Rosali *et al.* (2015) (Table 1).

MATERIALS AND METHODS

Problem formulation: Consider the steady two-dimensional boundary layer flow near the stagnation point over a permeable stretching/shrinking surface in a water based nanofluid containing two types of nanoparticles; Copper (Cu) and silver (Ag). The nanofluid is assumed to be incompressible and the effects of dissipation and radiation are neglected. The base fluid (water) and the nanoparticles are assumed to be in thermal equilibrium and no slip occurs between them. Table 2 displays the thermophysical properties of fluid and nanoparticles. Under these assumptions and following the model equations of nanofluid proposed by Tiwari and Das (2007), the governing boundary layer equations for the problem under consideration can be written as the following:

$$\frac{\partial u}{\partial x} + \frac{\partial v}{\partial y} + \frac{\partial w}{\partial z} = 0 \tag{1}$$

$$u \frac{\partial u}{\partial x} + v \frac{\partial u}{\partial y} + w \frac{\partial u}{\partial z} = u_e \frac{du_e}{dx} + v_{nf} \frac{\partial^2 u}{\partial z^2} \tag{2}$$

$$u \frac{\partial T}{\partial x} + v \frac{\partial T}{\partial y} + w \frac{\partial T}{\partial z} = \alpha_{nf} \frac{\partial^2 T}{\partial z^2} \tag{3}$$

Subject to the boundary conditions:

$$\begin{aligned} u = u_w(x) = ax, \quad v = 0, \quad w = w_w, \quad T = T_w \quad \text{at } z = 0, \tag{4} \\ u = u_e(x) = cx, \quad T = T_\infty \quad \text{as } z \rightarrow \infty \end{aligned}$$

Table 2: Thermophysical properties of fluid and nanoparticles (Abu-Nada and Oztop (2009))

Physical properties	Fluid phase (water)	Cu	Ag
C _p (J/kg K)	4179	385	235
ρ (kg/m ³)	997.1	8933	10500
k (kg/m ²)	0.613	400	429

where, x and y are the Cartesian coordinates with x and y in the plane of the stretching/shrinking sheet (z = 0) while the z-coordinate being measured normal to the stretching/shrinking sheet, u, v and w are the velocity components along the x, y and z, respectively, w_w is the mass flux velocity with w_w<0 for suction and w_w>0 for injection, T is the non-dimensional temperature of the nanofluid, T_w is the constant surface temperature distribution, T_∞ is the uniform temperature of the ambient nanofluid, u_w(x) is the velocity of the stretching/shrinking sheet, u_e(x) is the velocity of the external flow (potential flow) of the nanofluid with c being a constant where, c>0 for a stretching sheet and c<0 for a shrinking sheet and α is a positive constant. Further, μ_{nf} is the effective viscosity of the nanofluid and α_{nf} is the thermal diffusivity of the nanofluid which are given in Table 2 and are defined as:

$$\begin{aligned} \mu_{nf} = \frac{\mu_f}{(1-\phi)^{2.5}}, \quad \alpha_{nf} = \frac{k_{nf}}{(\rho C_p)_{nf}}, \quad \frac{k_{nf}}{k_f} = \frac{k_s + 2k_f - 2\phi(k_f - k_s)}{k_s + 2k_f + \phi(k_f - k_s)} \tag{5} \\ (\rho C_p)_{nf} = (1-\phi)(\rho C_p)_f + \phi(\rho C_p)_s, \quad \rho_{nf} = (1-\phi)\rho_f + \phi\rho_s \end{aligned}$$

where, φ is the nanoparticle volume fraction, ρ_{nf} is the effective density of the nanofluid, (ρC_p)_{nf} is the heat capacity of the nanofluid, k_{nf} is the effective thermal conductivity of the nanofluid, ρ_f is the reference density of the fluid fraction, ρ_s is the reference density of the solid fraction, μ_f is the viscosity of the fluid fraction, k_f is the thermal conductivity of the fluid, k_s is the thermal conductivity of the solid, (ρC_p)_f is the heat capacity of the fluid and (ρC_p)_s is the heat capacity of the solid. Following Miklavcic and Wang (2006) and Arifin *et al.* (2011), the similarity solutions of Eq. 1-3 are expressed in terms of the following variables:

$$\begin{aligned} u = cxf'(\eta), \quad v = c(m-1)yf'(\eta), \quad w = -\sqrt{cv}mf(\eta), \tag{6} \\ \theta(\eta) = \frac{T-T_\infty}{T_w-T_\infty}, \quad \eta = \sqrt{\frac{c}{v}}z \end{aligned}$$

where, primes denote differentiation with respect to η. Here, we have m = 1 when the sheet shrinks in the x-direction only and m = 2 when the sheet shrinks axisymmetrically. Equation 1 is automatically satisfied

while substituting 6 into Eq. 2 and 3 reduce the basic equations to the following ordinary differential equations:

$$\kappa_1 f''' + mf f'' + 1 - f'^2 = 0 \tag{7}$$

$$\kappa_2 \theta'' + Pr mf \theta' = 0 \tag{8}$$

while the boundary conditions Eq. 4 become:

$$\begin{aligned} f(0) = s, f'(0) = \lambda, \theta(0) = 1 \\ f'(\eta) \rightarrow 1, \theta(\eta) \rightarrow 0 \text{ as } \eta \rightarrow \infty \end{aligned} \tag{9}$$

Here, $Pr = \nu_f/\alpha_f$ is the Prandtl number, $s = -w_{\infty}/(c\nu_f)^{1/2}$ is the suction ($s>0$) parameter, $\lambda = \alpha/c$ is the stretching ($\lambda>0$) or shrinking ($\lambda<0$) parameter and κ_1 and κ_2 are two constants relating to the properties of the nanofluid which are defined as:

$$\kappa_1 = \frac{1}{(1-\phi)^{2.5} (1-\phi + \phi \rho_s/\rho_f)}, \kappa_2 = \frac{\kappa_{nf}/\kappa_f}{(1-\phi) + (\phi(\rho C_p)_s/(\rho C_p)_f)} \tag{10}$$

The physical quantities of interest are the skin friction coefficient C_f and the local Nusselt number Nu which are given by:

$$Re_x^{1/2} C_f = \frac{1}{(1-\phi)^{2.5}} f''(0), Re_x^{1/2} Nu_x = -\frac{k_{nf}}{k_f} \theta'(0) \tag{11}$$

where, $Re_x = u_e(x)x/\nu$ is the local Reynolds number.

Stability analysis: In the earlier study, we have mentioned the existence of dual solutions. In order to determine which of these solutions are physically realizable in the real world applications, we have to perform a stability analysis. This analysis has been performed by many researchers such as Weidman *et al.* (2006), Harris *et al.* (2009), Weidman and Sprague (2011) and most recently by Akbar *et al.* (2017) and Najib *et al.* (2018). First, we have to consider the unsteady problem. Equation 1 holds while Eq. 2 and 3 become:

$$\frac{\partial u}{\partial t} + u \frac{\partial u}{\partial x} + v \frac{\partial u}{\partial y} + w \frac{\partial u}{\partial z} = u_e \frac{du_e}{dx} + \nu_{nf} \frac{\partial^2 u}{\partial z^2} \tag{12}$$

$$\frac{\partial T}{\partial t} + u \frac{\partial T}{\partial x} + v \frac{\partial T}{\partial y} + w \frac{\partial T}{\partial z} = \alpha_{nf} \frac{\partial^2 T}{\partial z^2} \tag{13}$$

where, t denotes the time. Based on Eq. 6 and following Weidman *et al.* (2006), we now introduce the following new dimensionless variable:

$$\begin{aligned} u = c\alpha \frac{\partial}{\partial \eta} f(\eta, \tau), v = c(m-1)y \frac{\partial}{\partial \eta} f(\eta, \tau), w = -(c\nu_f)^{1/2} mf(\eta, \tau) \\ \theta(\eta, \tau) = (T-T_{\infty})/(T_w-T_{\infty}), \eta = (c\nu_f)^{1/2} z, \tau = ct \end{aligned} \tag{14}$$

where τ is a dimensionless time variable. Substituting Eq. 14 into 12 and 13 yield the following:

$$\kappa_1 \frac{\partial^3 f}{\partial \eta^3} + mf \frac{\partial^2 f}{\partial \eta^2} + 1 \left(\frac{\partial f}{\partial \eta} \right)^2 - \frac{\partial^2 f}{\partial \eta \partial \tau} = 0 \tag{15}$$

$$\kappa_2 \frac{1}{Pr} \frac{\partial^2 \theta}{\partial \eta^2} + mf \frac{\partial \theta}{\partial \eta} - \frac{\partial \theta}{\partial \tau} = 0 \tag{16}$$

which is subject to the boundary conditions:

$$\begin{aligned} f(0, \tau) = s, \frac{\partial}{\partial \eta} f(0, \tau) = \lambda, \theta(0, \tau) = 1 \\ \frac{\partial}{\partial \eta} f(\eta, \tau) \rightarrow 1, \theta(\eta, \tau) \rightarrow 0 \text{ as } \eta \rightarrow \infty \end{aligned} \tag{17}$$

To determine the stability of the solution $f = f_0(\eta)$ and $\theta = g_0(\eta)$ satisfying the boundary value problem Eq. 7-9, we write:

$$f(\eta, \tau) = f_0(\eta) + e^{-\gamma t} F(\eta, \tau), \theta(\eta, \tau) = g_0(\eta) + e^{-\gamma t} G(\eta, \tau) \tag{18}$$

where, γ is an unknown eigenvalue and $F(\eta, \tau)$ and $G(\eta, \tau)$ are small relative to $f_0(\eta)$ and $g_0(\eta)$. Solutions of the eigenvalue problem Eq. 15-17 give an infinite set of eigenvalues $\gamma_1 < \gamma_2 < \dots$, if the smallest eigenvalue γ_1 is positive, there is an initial decay which indicates that the flow is stable, however, if γ_1 is negative there is an initial growth of disturbances which indicates that the flow is unstable (Weidman and Sprague (2011)). Substituting Eq. 18 into 15 and 16, we obtain the following linearized problem:

$$\kappa_1 \frac{\partial^3 F}{\partial \eta^3} + m \left(f_0 \frac{\partial^2 F}{\partial \eta^2} + f_0'' F \right) - \left(2f_0' - \gamma \right) \frac{\partial F}{\partial \eta} - \frac{\partial^2 F}{\partial \eta \partial \tau} = 0 \tag{19}$$

$$\kappa_2 \frac{1}{Pr} \frac{\partial^2 G}{\partial \eta^2} + m \left(f_0 \frac{\partial G}{\partial \eta} + F g_0' \right) + \gamma G - \frac{\partial G}{\partial \tau} = 0 \tag{20}$$

Subject to the following boundary conditions:

$$\begin{aligned}
 F(0, \tau) = 0, \frac{\partial}{\partial \eta} F(0, \tau) = 0, G(0, \tau) = 0 \\
 \frac{\partial}{\partial \eta} F(\eta, \tau) \rightarrow 0, G(\eta, \tau) \rightarrow 0 \text{ as } \eta \rightarrow \infty
 \end{aligned}
 \tag{21}$$

By setting $\tau = 0$, we obtain the solutions $f(\eta) = f_0(\eta)$ and $\theta(\eta) = g_0(\eta)$. Hence, $F = F_0(\eta)$ and $G = G_0(\eta)$ in Eq. 19 and 20 identify initial growth or decay of the solution Eq. 18. To test our numerical procedure, we have to solve the following linear eigenvalue problem:

$$\kappa_1 F_0''' + m(f_0 F_0'' + f_0'' F_0) - (2f_0' - \gamma) F_0' = 0
 \tag{22}$$

$$\kappa_2 G_0'' + Pr m(f_0 G_0' + F_0 g_0') + \gamma G_0 = 0
 \tag{23}$$

Along with the boundary conditions:

$$\begin{aligned}
 F_0(0) = 0, F_0'(0) = 0, G_0(0) = 0 \\
 F_0'(\eta) \rightarrow 0, G_0(\eta) \rightarrow 0 \text{ as } \eta \rightarrow \infty
 \end{aligned}
 \tag{24}$$

It should be stated that for particular cases of λ , s , m and Pr , the stability of the corresponding steady laminar flow solutions $f_0(\eta)$ and $g_0(\eta)$ are determined by the smallest eigenvalue γ . Harris *et al.* (2009) suggested that the range of possible eigenvalues can be determined by relaxing a boundary condition on $F_0(\eta)$ or $G_0(\eta)$. Therefore, for the present problem, we relax the condition that $F_0'(\eta) \rightarrow 0$ as $\eta \rightarrow \infty$ and for a fixed value of γ we solve the system Eq. 22-23 along with the new boundary condition $F_0''(0) = 1$.

RESULTS AND DISCUSSION

Numerical solutions to the nonlinear ordinary differential Eq. 7 and 8 along with the boundary conditions Eq. 9 were obtained using the “bvp4c” function in MATLAB Kierzenka and Shampine (2001) for different values of the nanoparticle volume fraction ϕ . Following Khanafer *et al.* (2003); Tiwari and Das (2007); Abu-Nada and Oztop (2009), we have considered the range of nanoparticle volume fraction as $0 \leq \phi \leq 0.2$. The Prandtl number Pr of the base fluid (water) is kept constant at 6.7850 throughout the study. The thermophysical properties of fluid and nanoparticles used in this study are given in Table 2. To verify the accuracy

Table 3: Values of $f'(0)$ for $\phi = 0$ for Cu nanoparticles with different m and $s = 0$

λ	Wang (2008)		Present	
	$m = 1$	$m = 2$	$m = 1$	$m = 2$
1	0.0000	0.0000	0.0000	0.0000
0	1.232588	1.311938	1.232588	1.311938
-1	1.32882	0.0000	1.32882	0.30360

Table 4: Values of λ_c for Cu nanoparticles for several values of m and s when $\phi = 0$

m	s	λ_c
1	0	-1.24658
	0.5	-1.58011
2	0.5	-1.52676
	0.8	-2.00922

Table 5: Smallest eigenvalues λ for Cu nanoparticles when $\phi = 0.1$ and different values of λ and s

λ	s	λ (Upper branch)	λ (Lower branch)
-1.2	0	0.5780	-0.5172
-1.4	0.3	0.4862	-0.4502
-1.5	0.4	0.1496	-0.1463
	0.5	0.8097	-0.7210
	0.6	1.1791	-1.0000

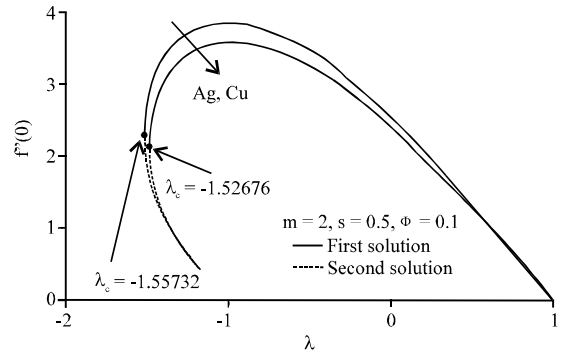


Fig. 1: Variation of $f''(0)$ with λ for different types of nanoparticles

of the present method, the present numerical results for $f''(0)$ are compared by Wang (2008) for various values of the stretching/shrinking parameter λ when $\phi = 0$ (regular Newtonian fluid). The comparisons which presented in Table 3 are found to be in very good agreement and thus, we are confident the present results are accurate.

Variation of the reduced skin friction coefficient $f''(0)$ and reduced local Nusselt number $-\theta'(0)$ with λ for different types of nanoparticles when $m = 2$, $s = 0.5$ and $\phi = 0.1$ are shown in Fig. 1 and 2, respectively. It seems that there are regions of unique solutions for $\lambda > -1$, dual solutions for $\lambda_c < \lambda < -1$ and no solution for $\lambda < \lambda_c$ where, λ_c is the critical value of λ beyond which the boundary layer separates from the surface and the solutions based upon the boundary-layer approximations are not possible. It is important to mention that in this study, the second

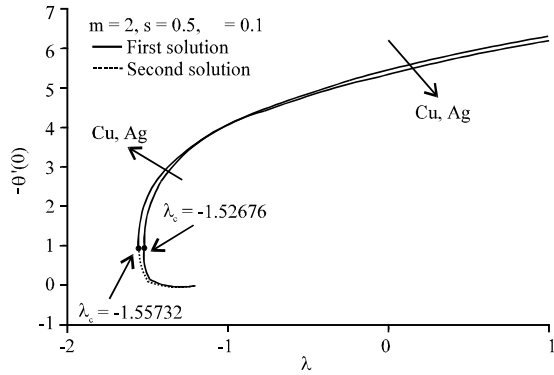


Fig. 2: Variation of $-\theta'(0)$ with λ for different types of nanoparticles

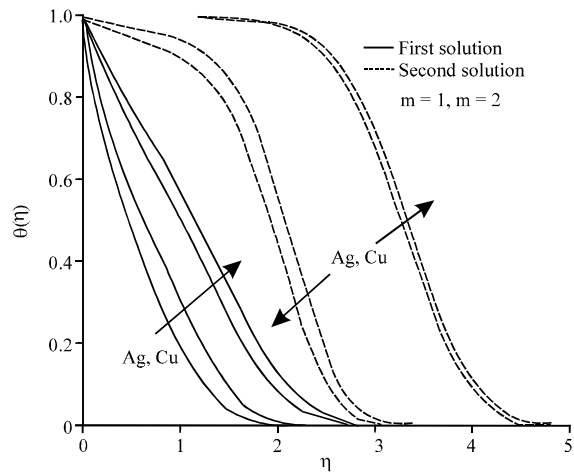


Fig. 4: Temperature profiles $\theta(\eta)$ for different types of nanoparticles when $m = 1$ and 2 , $s = 0.5$, $\lambda = -1.5$ and $\phi = 0.1$

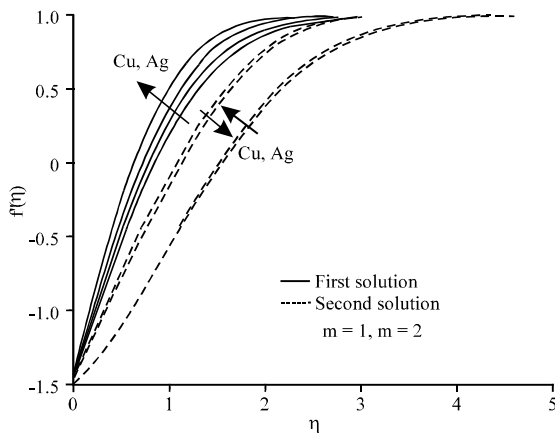


Fig. 3: Velocity profiles $f'(\eta)$ for different types of nanoparticles when $m = 1$ and 2 , $s = 0.5$, $\lambda = -1.5$ and $\phi = 0.1$

solutions only occur for the shrinking ($\lambda < 0$) case. Several values of λ_c for Cu nanoparticles for different m and s when, $\phi = 0.1$ are displayed in Table 4 and 5. From Fig. 1, it can be seen that the values of the reduced skin friction coefficient $f'(0)$ for nanoparticle Ag are higher than Cu while opposite behavior can be observed in Fig. 2, specifically when $\lambda > -1$. From Table 4, we found that the values of $|\lambda_c|$ increase with the increase of s . Hence, the suction parameter widens the range of λ for which the solutions exist.

Figure 3 and 4 display the velocity $f'(\eta)$ and temperature profiles $\theta(\eta)$ for both Cu and Ag nanoparticles for $m = 1$ (when the sheet shrinks in the x -direction only) and $m = 2$ (when the sheet shrinks axisymmetrically) when $s = 0.5$, $\lambda = -1.05$ and $\phi = 0.1$. The first (upper branch) solution and second (lower branch) solution are illustrated with solid and dashed lines, respectively. It is seen that the boundary layer thickness

of Cu nanoparticles is larger compared to Ag nanoparticles. Further, it can be observed in Fig. 4 that the heat transfer rate at the surface for Ag nanoparticles is higher than Cu. The boundary layer thickness for the second (lower branch) solution is seen to be larger than the first (upper branch) solution in both figures. Both velocity and temperature profiles displayed in Fig. 3 and 4 satisfy the far field boundary conditions asymptotically and thus, support the validity of the dual solutions obtained in this study.

Finally, a stability analysis was performed by solving an unknown eigenvalue γ on Eq. 22-23 along with the boundary conditions Eq. 24. The smallest eigenvalues γ for some values of γ and s are shown in Table 5. From the table, it can be seen that the upper branch solutions have positive eigenvalues γ while the lower branch have negative eigenvalues γ , thus, we conclude that the first (upper branch) solution is stable while the second (lower branch) solution is unstable.

CONCLUSION

The problem of boundary layer flow and heat transfer near the stagnation point past a permeable stretching/shrinking sheet in a nanofluid is investigated. The nonlinear ordinary differential equations are solved numerically for 2 types of nanoparticles which are copper (Cu) and silver (Ag) in the base fluid of water with Prandtl number kept constant to $Pr = 6.8750$. Results of the skin friction coefficients, local Nusselt numbers as well as the velocity and temperature profiles are presented and discussed for different values

of the governing parameters. Dual solutions are found for a certain range of shrinking and suction parameters and therefore, a stability analysis has been performed to determine which solution is stable and physically realizable. It can be concluded that the first (upper branch) solution is stable while the second (lower branch) solution is unstable.

ACKNOWLEDGEMENT

The researchers gratefully acknowledged the financial support received in the form of research university grant (GP-IPM/2018/9619000) from the Universiti Putra Malaysia.

REFERENCES

- Abu-Nada, E. and H.F. Oztop, 2009. Effects of inclination angle on natural convection in enclosures filled with Cu-water nanofluid. *Int. J. Heat Fluid Flow*, 30: 669-678.
- Akbar, T., S. Batool, R. Nawaz and Q.M.Z. Zia, 2017. Magneto-hydrodynamics flow of nanofluid due to stretching/shrinking surface with slip effect. *Adv. Mech. Eng.*, 9: 1-11.
- Arifin, N.M., R. Nazar and I. Pop, 2011. Viscous flow due to a permeable stretching/shrinking sheet in a nanofluid. *Sains Malaysiana*, 40: 1359-1367.
- Bakar, N.A.A., N. Bachok and N.M. Arifin, 2017. Rotating flow over a shrinking sheet in nanofluid using Buongiorno model and thermophysical properties of nanoliquids. *J. Nanofluids*, 6: 1215-1226.
- Bhattacharyya, K., T. Hayat and A. Alsaedi, 2013. Analytic solution for magneto-hydrodynamic boundary layer flow of Casson fluid over a stretching/shrinking sheet with wall mass transfer. *Chin. Phys. B*, Vol. 22, 10.1088/1674-1056/22/2/024702
- Choi, S.U.S., 1995. Enhancing Thermal Conductivity of Fluids with Nanoparticles. In: *Developments and Applications of Non-Newtonian Flows*, Siginer, D.A. and H.P. Wang (Eds.). ASME, New York, USA., pp: 99-105.
- Das, S.K., S.U.S. Choi, W. Yu and T. Pradeep, 2008. *Nanofluids: Science and Technology*. John Wiley & Sons, Hoboken, New Jersey, USA., ISBN:978-0-470-07473-2, Pages: 396.
- Daungthongsuk, W. and S. Wongwises, 2007. A critical review of convective heat transfer of nanofluids. *Renewable Sustainable Energy Rev.*, 11: 797-817.
- Fan, J. and L. Wang, 2011. Erratum: Review of heat conduction in nanofluids. *J. Heat Transfer*, 133: 1-1.
- Harris, S.D., D.B. Ingham and I. Pop, 2009. Mixed convection boundary-layer flow near the stagnation point on a vertical surface in a porous medium: Brinkman model with slip. *Trans. Porous Media*, 77: 267-285.
- Kakac, S. and A. Pramuanjaroenkij, 2009. Review of convective heat transfer enhancement with nanofluids. *Int. J. Heat Mass Transfer*, 52: 3187-3196.
- Khanafar, K., K. Vafai and M. Lightstone, 2003. Buoyancy-driven heat transfer enhancement in a two-dimensional enclosure utilizing nanofluids. *Int. J. Heat Mass Transfer*, 46: 3639-3653.
- Kierzenka, J. and L.F. Shampine, 2001. A BVP solver based on residual control and the MALTAB PSE. *ACM. Trans. Math. Software*, 27: 299-316.
- Miklavcic, M. and C.Y. Wang, 2006. Viscous flow due to a shrinking sheet. *Quart. Applied Math.*, 64: 283-290.
- Muthamilselvan, M., P. Kandaswamy and J. Lee, 2010. Heat transfer enhancement of copper-water nanofluids in a lid-driven enclosure. *Commun. Nonlinear Sci. Numer. Simul.*, 15: 1501-1510.
- Najib, N., N. Bachok, N.M. Arifin and F.M. Ali, 2018. Stability analysis of stagnation-point flow in a nanofluid over a stretching/shrinking sheet with second-order slip, Soret and Dufour effects: A revised model. *Appl. Sci.*, 8: 1-13.
- Nazar, R., M. Jaradat, N. Arifin and I. Pop, 2011. Stagnation-point flow past a shrinking sheet in a nanofluid. *Open Phys.*, 9: 1195-1202.
- Nield, D.A. and A.V. Kuznetsov, 2009. The Cheng-Minkowycz problem for natural convective boundary-layer flow in a porous medium saturated by a nanofluid. *Int. J. Heat Mass Transfer*, 52: 5792-5795.
- Noor, N.F.M. and I. Hashim, 2009. MHD flow and heat transfer adjacent to a permeable shrinking sheet embedded in a porous medium. *Sains Malaysiana*, 38: 559-565.
- Rosali, H., A. Ishak, R. Nazar and I. Pop, 2015. Rotating flow over an exponentially shrinking sheet with suction. *J. Mol. Liq.*, 211: 965-969.
- Sajid, M., T. Hayat and T. Javed, 2008. MHD rotating flow of a viscous fluid over a shrinking surface. *Nonlinear Dyn.*, 51: 259-265.
- Tham, L., R. Nazar and I. Pop, 2012. Mixed convection boundary layer flow from a horizontal circular cylinder in a nanofluid. *Intl. J. Numer. Methods Heat Fluid Flow*, 22: 576-606.

- Tiwari, R.K. and M.K. Das, 2007. Heat transfer augmentation in a two-sided lid-driven differentially heated square cavity utilizing nanofluids. *Int. J. Heat Mass Transfer*, 50: 2002-2018.
- Uddin, M.J., W.A. Khan and A.M. Ismail, 2018. Melting and second order slip effect on convective flow of nanofluid past a radiating stretching/shrinking sheet. *Propul. Power Res.*, 7: 60-71.
- Vajjha, R.S. and D.K. Das, 2012. A review and analysis on influence of temperature and concentration of nanofluids on thermophysical properties, heat transfer and pumping power. *Int. J. Heat Mass Transfer*, 55: 4063-4078.
- Wang, C.Y., 2008. Stagnation flow towards a shrinking sheet. *Intl. J. Non Linear Mech.*, 43: 377-382.
- Wang, X.Q. and A.S. Mujumdar, 2008. A review on nanofluids-part I: Theoretical and numerical investigations. *Braz. J. Chem. Eng.*, 25: 613-630.
- Weidman, P.D. and M.A. Sprague, 2011. Flows induced by a plate moving normal to stagnation-point flow. *Acta Mech.*, 219: 219-229.
- Weidman, P.D., D.G. Kubitschek and A.M.J. Davis, 2006. The effect of transpiration on self-similar boundary layer flow over moving surfaces. *Int. J. Eng. Sci.*, 44: 730-737.